HiSST: 3rd International Conference on High-Speed Vehicle Science Technology

14 -19 April 2024, Busan, Korea

System Study of an Integrated Facility with Arc-Jet and Expansion Tube for Hypervelocity Testing with Ablating Spacecraft Models

Eric Won Keun Chang[1], Tobias A. Hermann[2]

Abstract

Ground testing for the atmospheric entry environment requires precise matching of key flow parameters. However, existing hypersonic facilities can only partially replicate some aspects of this complex environment. Plasma wind tunnels can generate continuous high-enthalpy flow, but challenges arise in achieving aerodynamic similarity. Impulse facilities can match the velocity and total pressure of hypersonic flow, but only for a short test duration. A hybrid facility allows a more comprehensive simulation of atmospheric entry conditions by using the small-scale thermal arc-jet Osney Plasma Generator (OPG) to heat the test model, which is then exposed to the hypervelocity flow generated from the Cold-Driven Expansion Tube (CXT). This paper presents a detailed system design study and discussion regarding the capability of an integrated arc-jet/expansion tube facility.

Keywords: *Ground Test Facilities, Impulse Facilities, Expansion Tube, Arc-jet, Ablation*

Nomenclature

a – Sound speed, m/s
H – Specific enthalpy, MJ/kg
L – Length, m
T – Temperature, K
p – Pressure, Pa
v – Velocity, m/s
ρ – Density, kg/m^3
$\dot{m}$ – Mass flow rate, g/s
U_e – flight equivalent velocity, km/s

Subscripts
∞ – Freestream, flight
1 – Shock tube
4 – Driver tube
5 – Acceleration tube
7 – Freestream, expansion tube
t – Total
opg – relating to plasma wind tunnel
cxt – relating to expansion tube
flight – flight equivalent
w – wall

1. Introduction

When a spacecraft re-enters the Earth's atmosphere, it encounters hypersonic airspeeds ranging from several to tens of kilometers per second [1]. Two types of ground testing facilities have been widely used in simulating these high velocity and enthalpy effects: impulse facilities and plasma wind tunnels. Each facility addresses separate aspects in the hypersonic test environment [2]. Impulse facilities can achieve total pressure and velocity experienced during flight, but they have a limited quasi-steady test time, allowing only tests up to milliseconds to be performed. On the other hand, plasma wind tunnels provide continuous test durations to simulate material response under high-enthalpy conditions. However, achieving aerodynamic similarity on a test model in these tunnels is challenging, as only the stagnation properties are commonly replicated.

[1] *Hypersonics Group, Oxford Thermofluids Institute, University of Oxford, ericwk.chang@eng.ox.ac.uk*
[2] *Hypersonics Group, Oxford Thermofluids Institute, University of Oxford, tobias.hermann@eng.ox.ac.uk*

For a complete simulation of critical flow properties, various methods have been developed to achieve model preheating in impulse facilities. Firstly, electrical preheating of resistive materials was developed at the University of Queensland and used for the testing of ablation [3] and simulating heated boundary layers in shock interactions [4]. Arc-jet heating, on the other hand, can produce mass blowing effect through pyrolysis and offers flexibility in model geometry and material [5]. In line with this, the small-scale arc-jet Osney Plasma Generator (OPG) [6,7] has recently been developed at the University of Oxford. The OPG arc-jet can serve as a preheating device for experiments in hypervelocity flows. Along with the OPG, the Cold-Driven Expansion Tube (CXT) is currently under construction to showcase the integration.

The integrated facility will enable a novel experimental ground testing methodology for ablating spacecraft heat shields in hypervelocity flows. The objective of this paper is to outline the integration process of OPG into a new expansion tube, with a discussion focusing on appropriate flow conditions in matching the key parameters in the experiment. Before moving into the experimental phase, this paper aims to outline a theoretical investigation, focusing on the system design study of integrating OPG and CXT, particularly in relation to the differing similarity theories. The purpose of this system design study is to explore the capabilities of the integrated facility based on the given setup. Firstly, the theoretical performance map of both OPG and CXT will be developed to investigate their individual experimental simulation capabilities. These will be backed up and improved by the actual facility data measured in the experiments.

2. Experimental Facilities

2.1. OPG Plasma Wind Tunnel

Osney Plasma Generator (OPG) [5-10] is a small-scale, 21.5 kW thermal arc-jet recently developed at the University of Oxford Hypersonics Group. Fig. 1 displays the photo of the OPG Plasma Wind Tunnel facility. Using a welding power supply, the plasma generator is powered up to 510 A DC. Two types of plasma generators have been developed and are currently operational. OPG1 is the first design, producing argon plasma flow through an axisymmetric converging-diverging nozzle geometry. OPG2 has been developed featuring a settling chamber for oxygen injection, enabling the generation of air composition plasma. Experimental photos of OPG1 and OPG2 testing showcase material testing using a spacecraft model and the production of N_2 and air plasma.

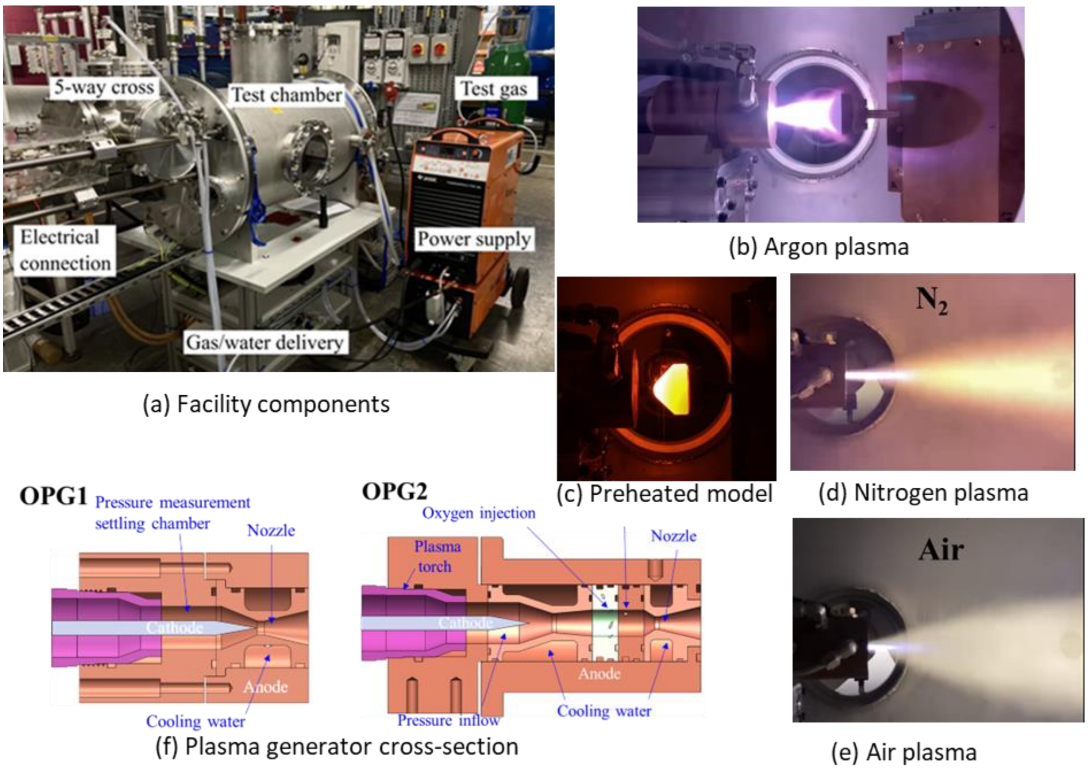

Fig 1. OPG Plasma Wind Tunnel Facility [5-10].

2.2. CXT Expansion Tube

The Cold-Driven Expansion Tube (CXT) is a new hypersonic test facility currently under construction at the University of Oxford. Fig.2 displays an overview of the CXT facility. The expansion tube has a length of approximately 12 m with an internal diameter of 177.8 mm. In contrast to the free-piston compression of T6 [9], CXT uses pressurized helium as a driver gas to produce flows from 2 to 6 km/s. When the facility is fired, the rupturing of the primary diaphragm generates a primary shock, which is then processed further by the unsteady expansion behind a secondary shock. The flow condition is determined by driver tube pressure p_4, shock tube pressure p_1 and acceleration tube pressure p_5, which are separated by primary and secondary diaphragms. Unlike reflected shock tunnels that generate a stagnant nozzle-supply flow, expansion tube flows involve unsteady expansion that adds complexity to the determination of the desired flow conditions for experimental testing.

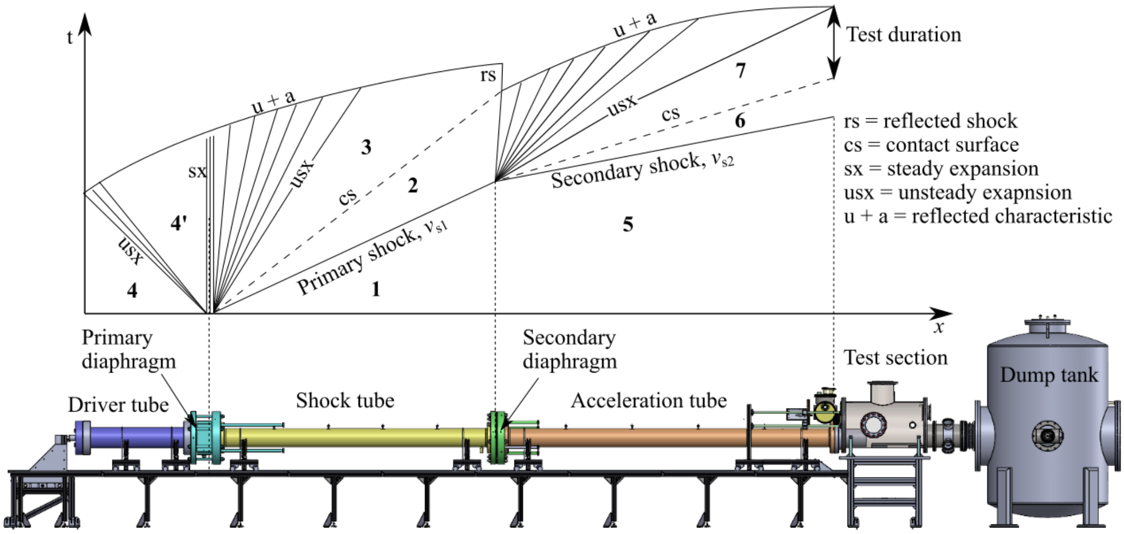

(a) CAD schematic and position-time (x-t) diagram

(b) CXT construction site

Fig 2. Cold-Driven Expansion Tube CXT.

3. Integrated Arc-jet and Expansion Tube Facility

Fig. 3 displays the CAD schematic of the arc-jet preheating apparatus in the CXT test section. The test section is configured to accommodate both the exit of the expansion tube and the OPG arc-jet plasma generator. The arc-jet is located parallel to the expansion tube, but within a separate isolated duct to prevent increase in chamber pressure (p_5), a critical parameter in generating expansion tube conditions. The plasma duct is sealed from the remaining test section to prevent entering cooled plasma test gas. The testing procedure starts with the arc-jet preheating of the test model. When the desired surface temperature (T_w) is attained, a pneumatic actuator quickly moves the test model to the exit of the expansion tube. Then, the expansion tube is fired to develop hypervelocity flow-field over an ablating test model.

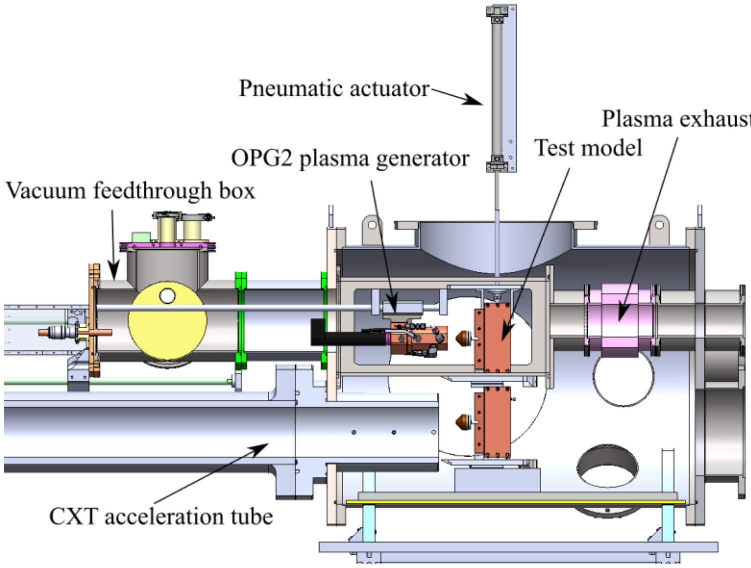

Fig. 3. Integrated arc-jet and expansion tube facility.

4. System Design Study

This section aims to present various aspects of the system study. First, the basic scaling parameters are outlined. To obtain these parameters, the process of establishing the baseline properties of the two different facilities is discussed. Then, the initial analysis was conducted involving a ground-to-flight extrapolation.

4.1. Target Flight Condition and Basic Scaling parameters

The achievable flow conditions of the integrated facility should be systematically studied prior to the development. Typical ballistic trajectory points could be used for the target conditions of the facility. Due to the finite size of the OPG and CXT core-flow, a sub-scale spacecraft model needs to be used for the experiment. Thus, an appropriate tunnel-to-flight conversion needs to be established with different scaling methodologies. Fig. 4 illustrates a schematic of the integrated facility, labeled with important experimental parameters. For the plasma side, the total enthalpy of the plasma ($H_{t,opg}$) is dictated by the input energy and mass flow rate ($\dot{m}$) to preheat the experimental model with radius R to raise the surface temperature (T_w). For the expansion tube side, the parameters include p_5, the test section pressure must be kept at a desired level before the shot depending on the value of p_5, The expansion tube produces flow with total enthalpy ($H_{t,cxt}$) and freestream density (ρ_7). Finally, the T_w achieved from a material sample will eventually need to match the wall-to-total temperature ratio ($T_w/T_{t,cxt}$) of the actual re-entry flight to simulate appropriate the ablation-coupled flow-field.

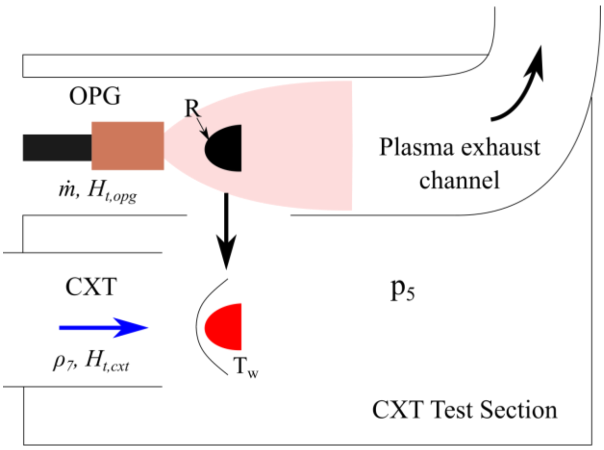

Fig. 4. Schematic of the integrated Facility. Reproduced from [6].

4.2. Plasma Flow Characterization

To characterize the performance of the generator, steady plasma flow conditions were generated using various DC current (A) and mass flow rate ($\dot{m}$) settings. A 15 mm exit diameter nozzle configuration was used for the current investigation. Using the measured data of the Pitot (stagnation) probe and a slug calorimeter [10], together with the radius of the probe as inputs for the ASTM method [12], the total enthalpy of the plasma ($H_{t,opg}$) was determined. Fig. 5 shows an example measurement of an Argon jet with Pitot (stagnation) pressure and calculated heat flux from a slug calorimeter at various current and mass flow rates. The steady Pitot pressure distribution taken at 200A shows a clear trend of pressure increasing with the mass flow rate. Additionally, for the heat flux rate, an increase in electrical power (from 300 to 500A) and mass flow rate leads to an increase in the heat flux rate to over 3 MW/m^2.

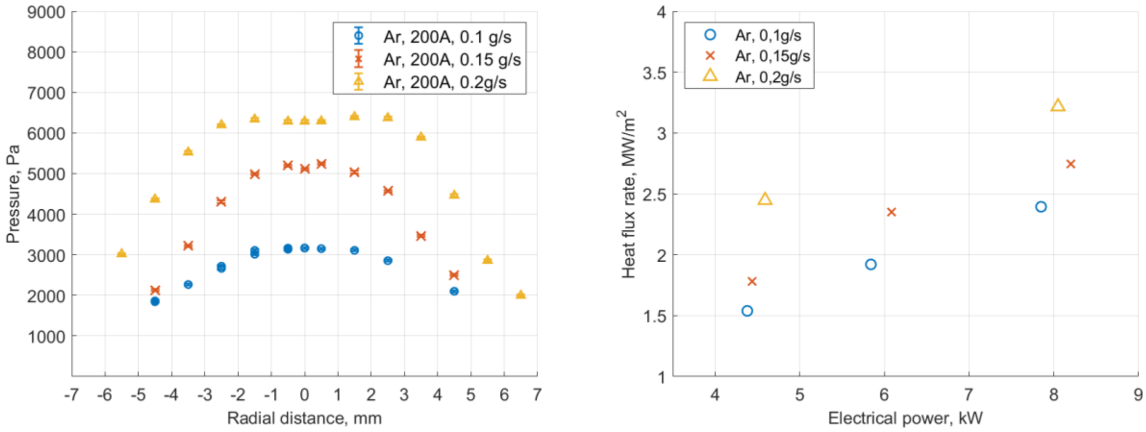

Fig. 5. Example Pitot pressure (left) and heat flux (right) results of the Argon plasma jet.

Using the centerline Pitot pressure (p_{pitot}) and placing the 15 mm diameter slug calorimeter in the same location, the total enthalpy ($H_{t,\,OPG}$) is determined using the ASTM method [12]. Table 1 and 2 list the various combinations of plasma input parameters, obtaining total enthalpy from 3 up to 6 MJ/kg with Argon, and 9 to over 14 MJ/kg with Nitrogen with the current experimental apparatus. Nitrogen plasma produces much higher heat flux/enthalpy than argon plasma due to higher voltage output occurring from electric energy transfer. Higher enthalpy can be produced by higher $\dot{m}$ and electric current. More datasets are currently being collected to test the full and potential envelope of the new plasma facility.

Table 1 Measured and calculated flow properties of Argon plasma jets.

Current, A	**$\dot{m}$, g/s**	**p_{pitot}, kPa**	**$\dot{q}$, MW/m^2**	**$H_{t,\,opg}$, MJ/kg**
200	0.1	3.16	1.14	3.19
300	0.15	5.20	1.78	3.88
400	0.15	5.30	2.35	5.07
500	0.15	5.51	2.74	5.80
500	0.2	7.32	3.24	5.95

Table 2 Measured and calculated flow properties of Nitrogen plasma jets.

Current, A	**$\dot{m}$, g/s**	**p_{pitot}, kPa**	**$\dot{q}$, MW/m^2**	**$H_{t,opg}$, MJ/kg**
200	0.1	3.48	2.23	8.99
200	0.15	5.11	3.67	12.17
300	0.15	5.20	4.35	14.22

4.3. Expansion Tube Conditions

The benefit of the expansion tube is in its near flight-duplicated flow speed and density capability. Designing the expansion tube flow conditions requires careful consideration due to the absence of gas stagnation within the facility. Typically, in an expansion tube experiment, the total enthalpy $H_{t,cxt}$ (which converts into flight-equivalent velocity U_e) and the ρL needs to be matched to retain binary scaling reactions for a subscale model. Scaling post-shock equilibrium density ρ_{eq} can normally be achieved much more easily than freestream density scaling in an expansion tube. This is due to the lower Mach number of the test conditions compared to flight, resulting in less total pressure being lost across the bow shock forms on the test model.

In contrast to using air as a typical accelerator tube gas in expansion tubes, the use of helium in CXT can enhance flow velocity and achieve a lower freestream temperature closer to the actual re-entry flights. This approach not only brings the hypervelocity freestream closer to equilibrium but also facilitates higher Mach numbers among conditions that allow for the possibility of achieving Mach number similarity. The smaller size of the model is advantageous with a smaller model length (radius) R for reaching higher T_w for ablation in OPG. For ρ-L scaling, however, a smaller size requires a much higher ρ_∞ to match binary-scaling in chemical reactions.

The PITOT3 [13] program was used to simulate the theoretical expansion tube conditions. Simulations were run using 'condition builder' mode to provide an envelope of possible conditions, with the driver gas pressure (p_4) set from 0.5 to 8 MPa while exploring different combinations of shock tube pressure p_1 and acceleration tube pressure p_5. p_1 varied from 1 to 50 kPa with an 11-species air mixture, and p_5 varied from 1 to 400 Pa with helium. The acceleration gas is set to expand to the velocity of the flow behind the secondary shock (v_6), hence effectively simulating as a conservative estimate in terms of achievable enthalpy. Table 3 shows example CXT flow conditions, which aims to produce a 4.7 km/s condition with the same enthalpy with a different freestream density. ρ-L scaling could be achieved by using different p_4 fill pressures, and theoretically, a model scaling factor of up to 14.8 could be obtained.

Table 3 Example CXT flow conditions calculated from PITOT3 simulations.

Properties	**p_4, MPa**	**p_1, kPa**	**p_5, Pa**	**$H_{t,cxt}$, MJ/kg**	**U_e, km/s**	**ρ_{7e}, kg/m^3**
Condition A	0.5	0.5	3	11.0	4.682	0.0081
Condition B	1	1	5	11.2	4.733	0.0144
Condition C	8	5	63	11.2	4.727	0.1198

Fig. 6 shows the variation in total enthalpy and equilibrium density at different p_1 and p_5 conditions. The trend indicates that an increase in p_5 leads to a decrease in total enthalpy of the expansion tube flow $H_{t,cxt}$, while increasing ρ_{7e}. Given a target $H_{t,cxt}$, a small test model requires generating a higher density to match ρ-L scaling. Achievable density is limited by the 8MPa fill condition. p_1 dictates the sound speed of the shocked test gas (a_2), which needs to be larger than the sound speed of the expanded driver gas (a_3) to ensure sufficient quasi-steady test time [14].

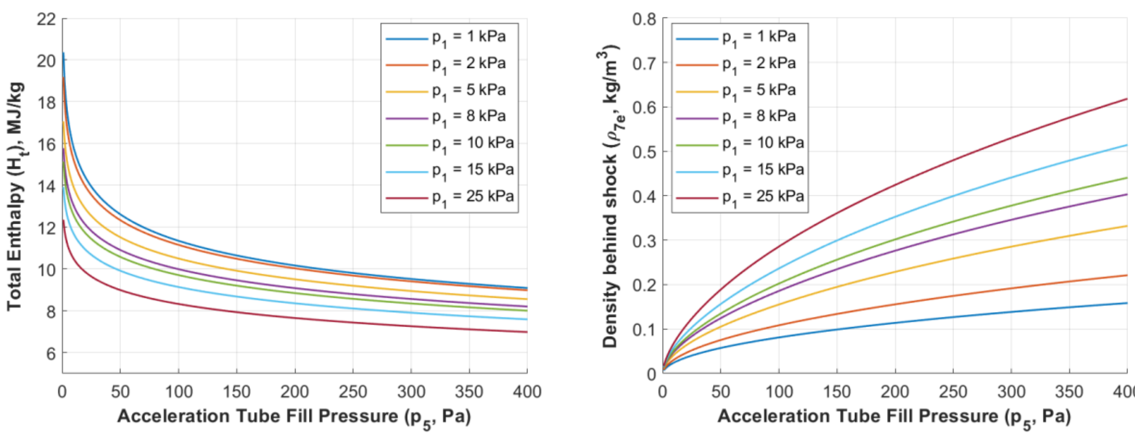

Fig 6. Total enthalpy and equilibrium density variation with different p_1 and p_5 fill conditions.

Another aspect of the flow acceleration from the expansion tube is that higher freestream temperatures are often achieved, leading to freestream flow in a nonequilibrium state. Fig. 7 illustrates the variation of freestream temperature and Mach number distribution with the acceleration tube fill pressure. To achieve Mach number scaling, it is best to keep the p_1 as high as possible while keeping the p_5 as low as possible. The trend observed in PITOT3 simulation indicates the characteristics of the freestream flow, hence it is important to choose the appropriate fill pressures to generate the test flow with sufficient quasi-steady test time.

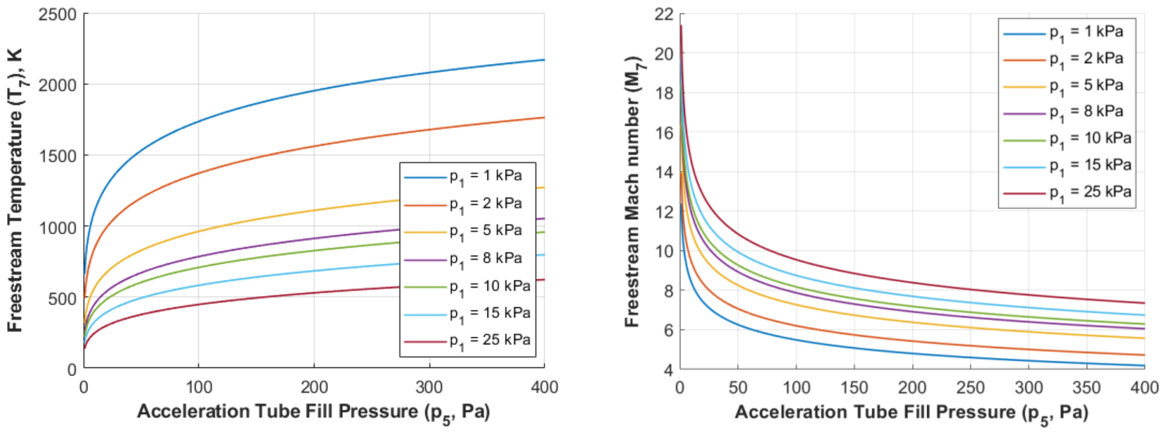

Fig 7. Freestream temperature and Mach number with different p_1 and p_5 fill conditions.

4.4. Ground-to-Flight Scaling Analysis

Next, the capability of the integrated arc-jet/expansion-tube facility is analyzed with an appropriate ground-to-flight extrapolation. The test model was assumed to have a scaling factor of 10, meaning the test model is 10 times smaller than the actual flight vehicle. For the plasma conditions, the Local Heat Transfer Simulation (LHTS) method [15] was employed to extrapolate the plasma flow to flight conditions using flow properties in Tables 1 and 2. The LHTS method aims to duplicate the flight by matching the total enthalpy of the plasma ($H_{t,opg}$), Pitot pressure of the plasma ($p_{pitot,opg}$), and the velocity gradient at the boundary layer edge (β).

For the current analysis, the scaling with the plasma flow utilized only the $H_{t,opg}$ and $p_{pitot,opg}$ values from Tables 1 and 2 to match the total enthalpy of flight $H_{t,flight}$ and Pitot pressure expected in flight $p_{pitot,flight}$. Using the definition of the total enthalpy, $H_{t,opg} = cp\ T_{flight} + U_{e,opg}^2/2$, the flight equivalent velocity of the plasma flow $U_{e,opg}$ could be obtained by assuming freestream temperature at 60-70 km altitude ($T_{flight} \approx 245$ K). The flight-equivalent Mach number (M_{flight}) could be attained using $U_{e,opg}/a_{flight}$. Then, using the M_{flight}, the $p_{pitot,opg}$ was used to find the flight equivalent freestream pressure, $p_{\infty,flight}$, which were then converted into the corresponding flight altitude using a 1976 US Standard Atmosphere database.

The binary scaling theory of the expansion tube facility assumes the product ρL to be constant while maintaining $H_{t,cxt}$. This means that smaller model sizes require higher freestream densities in the facility compared to the actual flight conditions. With a scaling factor of 10, CXT utilizes density 10 times higher than that of the flight-equivalent density. Thus, the flight-equivalent density is 10 times smaller, adjusting the flight density altitude accordingly. Fig. 8 displays an altitude-velocity map featuring the converted plasma flow properties and PITOT3 simulation results of CXT flight altitude (determined from freestream density) and flight-equivalent velocity (U_e) at 0.5 and 8 MPa driver tube fill pressures, alongside with various re-entry trajectories. A potential matching between the CXT and OPG N_2 plasma conditions could be achieved at Lower p_5 fill pressures. This also could simulate Space Shuttle peak heating. Higher p_5 fill pressures could simulate the lower end of Mars/Lunar return and boost-glide vehicle trajectories. Furthermore matching CXT flow with OPG Ar conditions could be achieved by employing 0.5MPa driver gas fill pressures.

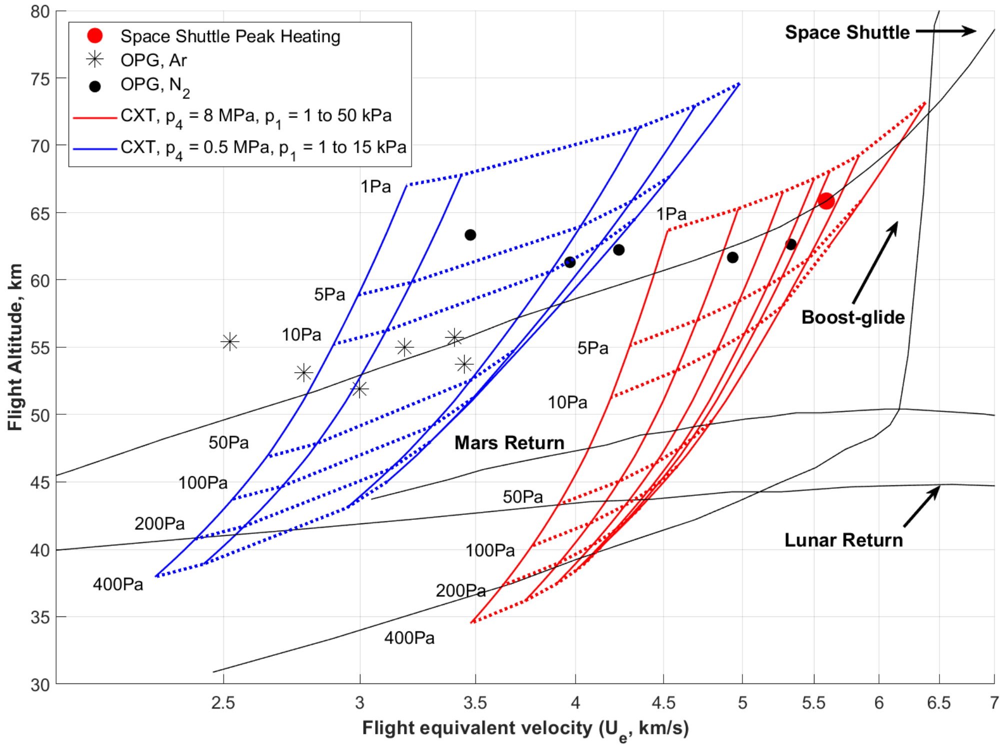

Fig 8. Altitude-Velocity map of the of the integrated facility. Horizontal isoline represents same p_5, vertical isoline represents same p_1. Trajectories reproduced from [11,16].

5. Conclusions

This study presents a system design aspect of an integrated arc-jet/expansion tube facility to estimate the theoretical envelope for determining achievable conditions in experiments. Utilizing the fundamental scaling laws of the plasma wind tunnel and the impulse facility, the first step involves scaling the total enthalpy and Pitot pressure of the plasma. Comparing these with the potential CXT envelope demonstrates their potential overlap, effectively matching key parameters for simulating hypervelocity environments. Future work on scaling will involve a full LHTS simulation with calculated velocity gradient. Also Adding more datasets (air) from the full characterization of the OPG plasma tunnel and conducting additional PITOT3 simulations with different driver gas fill conditions. The ongoing experimental material tests will indicate the maximum temperature of the preheated samples. Lastly, theoretical envelope will eventually be validated with actual CXT experimental data, providing a more comprehensive picture of achievable conditions.

6. Acknowledgements

This research was funded by the UKRI Future Leaders Fellowship scheme (grant number MR/T041269/1), and we extend our gratitude to UKRI. For Open Access, the author has applied for a CC BY public copyright license to any Author Accepted Manuscript (AAM) version arising from this submission. The authors also acknowledge Dr Chris James of the University of Queensland for his valuable discussions and assistance with PITOT3 simulations.

References

1. Park, C.: Review of chemical-kinetic problems of future NASA missions. I-Earth entries. Journal of Thermophysics and Heat Transfer (1993). https://doi.org/10.2514/3.431

2. Lu, F. and Marren, D.E.: Advanced Hypersonic Test Facilities, Boston (2002)
3. Lewis, S.W., Lewis, S. W., James, C. M., Ravichandran, R., Morgan, R. G., and McIntyre, T. J.:Carbon Ablation in Hypervelocity Air and Nitrogen Shock Layers. Journal of Thermophysics and Heat Transfer (2018). https://doi.org/10.2514/1.T5270
4. Chang, E.W.K., Chang, E. W. K., Chan, W. Y. K., McIntyre, T. J., and Veeraragavan, A.: Hypersonic shock impingement on a heated flat plate at Mach 7 flight enthalpy. Journal of Fluid Mechanics (2021). https://doi.org/10.1017/jfm.2020.877
5. Chang, E. W. K., Joglekar, C., McGilvray, M., and Hermann, T. A.: "Integration of Arc-jet in Impulse Facility for Hypervelocity Aerothermal Testing with Ablation. AIAA SciTech Forum (2023). https://doi.org/10.2514/6.2023-2334.
6. Hermann, T. A, Chang, E. W. K., Schäfer, J., Joglekar, C., and Böhrk, H.: "Development of Small Scale Arc-jet Facility OPG1. AIAA SciTech Forum (2023). https://doi.org/10.2514/6.2023-2331.
7. Chang, E. W.K., Schäfer, J., Valeinis, O., Buquet, M.T.B., Hermann, T. A, "Commissioning the OPG1 Plasma Wind Tunnel." Proceedings of ISSW 2023.
8. Schäfer, J., Chang, E. W. K., Hermann T. A., Loehle, S.: "Experimental Investigation of a Small-scale Arc-jet for Earth Entry Simulation." AIAA SciTech Forum (2024). https://doi.org/10.2514/6.2024-2571.
9. Buquet, M. T. B., Chang, E. W. K., Williams, B. A., Hermann T. A.: "Experimental Characterization of a Small Scale Arc-Jet Flow Using a Spatially Resolved UV-nIR Spectroscopy System." AIAA SciTech Forum (2024). https://doi.org/10.2514/6.2024-2212.
10. Valeinis O., Chang, E. W. K., Hermann T. A.: "Development and Testing of Slug Calorimeter and Total Pressure Probes for a Miniaturized Arc-jet." AIAA SciTech Forum (2024). https://doi.org/10.2514/6.2024-2886.
11. Collen, P., Doherty, L. J., Hambidge, C., Morgan, R., and McGilvray, M.: Development and commissioning of the T6 Stalker Tunnel. Experiments in Fluids (2021). https://doi.org/10.1007/s00348-021-03298-1.
12. ASTM International, Standard Test Method for Calculation of Stagnation Enthalpy from Heat Transfer Theory and Experimental Measurements of Stagnation-Point Heat Transfer and Pressure. Tech. Rep. E637-05 (2005).
13. James, C. M., Gildfind, D. E., Lewis, S. W., Morgan, R. G., Zander, F.: Implementation of a state-to-state analytical framework for the calculation of expansion tube flow properties. Shock Waves (2018). https://doi.org/10.1007/s00193-017-0763-3
14. Paull, A., Stalker, R.J.: Test flow disturbances in an expansion tube. Journal of Fluid Mechanics (1992). doi:10.1017/S0022112092000569
15. Kolesnikov, A.F.: Extrapolation from high enthalpy tests to flight based on the concept of local heat transfer simulation. In: Measurement Techniques for High Enthalpy and Plasma Flows, 8B. VKI, RTO (1999).
16. Acton, J. M., "Hypersonic Boost-Glide Weapons," Science & Global Security, Vol. 23, No. 3, Sep 2015, pp. 191–219.